J Fluoresc (2013) 23:1217–1227
DOI 10.1007/s10895-013-1252-4

ORIGINAL PAPER

Probing the Microscopic Aspects of 1-Butyl-3-Methylimidazolium Trifluoroacetate Ionic Liquid and Its Mixture with Water and Methanol: A Photophysical and Theoretical (DFT) Study

Sudhir Kumar Das · Prabhat Kumar Sahu · Moloy Sarkar

Received: 29 March 2013 / Accepted: 17 June 2013 / Published online: 29 June 2013

Abstract Considering the potential of mixed ionic liquid-cosolvent systems in wide range of applications, photophysical and theoretical studies on an industrially important ionic liquid, 1-butyl-3-methylimidazolium trifluoroacetate (BMIMTFA), and also its mixture with water and methanol have been investigated. Two organic dipolar solutes coumarin 153 (C153) and 2-aminonitrofluorene (ANF) have been used as the probe molecule for the present study. Steady-state absorption and emission spectral behavior of C153 has not been significantly influenced by both the cosolvents. However, excitation wavelength dependent measurements with ANF in the BMIMTFA-water and BMIMTFA-methanol show entirely different photophysical response. For BMIMTFA-methanol system the average solvation and rotational time is found to be less than that in BMIMTFA-water system. Quite interestingly, time-resolved fluorescence anisotropy measurements reveal two different solute-solvent coupling constant (C_{obs}) even if same mole fraction of water and methanol is used for the mixed solvent systems. Theoretical calculations also reveal stronger intermolecular interaction between IL and methanol than that between IL and water. The present combined photophysical and theoretical calculations seem to suggest different microscopic structural organization in the two binary systems.

Keywords Ionic liquids · Fluorescence · Excitation wavelength dependence · Binary mixtures · Structural organization

S. K. Das · P. K. Sahu · M. Sarkar (✉)
School of Chemical Sciences, National Institute of Science Education and Research, Bhubaneswar 751005, India
e-mail: moloysarkar@gmail.com

Introduction

Room temperature ionic liquids (RTILs) continue to attract considerable attention of the academic and industrial communities for quite some time due to their interesting physical attributes such as low vapor pressure, wide liquid range, moderate-to-high viscosity, etc. [1–4]. They are being used in a large number of applications in organic synthesis, catalysis, material science, and biosynthesis [1–3]. However, the ILs are not easily available like common solvents and are also expensive. Hence, the scale at which the neat IL should be used in the practical applications has not been reached till date. One of the possible approaches to expand the uses of RTILs would be to use binary and ternary mixtures of RTILs with various cosolvents. IL-cosolvent mixtures are also known to exhibit interesting physicochemical properties [5, 6]. However, a deeper understanding of their physicochemical properties in terms of IL-cosolvent interactions is extremely important so that the systems be used in more effective manner.

Recently, several studies have been carried out to understand the physicochemical properties of the mixtures of RTILs and conventional solvents. These studies have revealed that the solvent property can be fine-tuned by the addition of conventional solvents which will eventually enhance the scope of the applications of the RTILs. It has been observed that the addition of a cosolvent into RTILs has profound influence in changing the physicochemical properties of RTILs such as viscosity, polarity, conductivity [7–14]. A few studies have also been carried out to find the effect of cosolvent on the solute and solvent dynamics [15–21]. Quite interestingly, these studies reveal that

presence of trace amount of organic cosolvents is capable of changing the local microenvironment of the probe molecule. Recent work by Sarkar and coworkers [19] have shown that the addition of water/organic solvent to 1-ethyl-3-methylimidazolium ethylsulfate (EMIMESU) RTIL, decreases the average rotational and solvation time of C153 due to the reduction of viscosity of the media. Effect of nonpolar cosolvent on IL has been studied by Samanta and coworkers [17], and also by us [21] independently. These studies reveal that nonpolar cosolvent can effectively penetrate into the cybotactic region of the probe molecule. A favorable lipophilic interaction between the IL and nonpolar cosolvent is found to be responsible for this behavior. The physicochemical properties of the ionic liquid depend on the constituents of the ionic liquids. Hence, different cosolvents are expected to interact differently with the constituent of the ionic liquid. Thus it is of paramount importance to study the effect of cosolvents by taking ionic liquid having different constituents. We would also like to point out that apart from the lowering of the average rotational and solvation time of probe due to the reduction of viscosity of the media not much physical insight has been obtained by earlier studies.

Keeping these in mind, we have carried out solute and solvent relaxation of coumarin153 (C153) in 1-butyl-3-methylimidazolium trifluoroacetate (BMIMTFA) and also its mixture with water and methanol. The choice of the ionic liquid is governed by the fact that the ionic liquid bearing the trifluoroacetate moiety has the tremendous potential to be used in several industrial applications [22, 23]. Moreover, trifluoroacetate (TFA) anion has favorable proton accepting site due to the presence of the carboxylate moiety, it is also expected that it would participate in hydrogen bonding interaction with the protic solvents [24] and thereby control the physiochemical property of the medium. It is pertinent to mention in this context that ionic liquids having trifluoroacetate moiety are hygroscopic in nature, and trifluoroacetate anion is primarily responsible for the water miscibility [10]. Considering the favorable interaction between TFA and polar protic solvents, we have chosen water and methanol as the cosolvents for the present study. We have chosen C153 as a probe for its suitable photophysical properties [25–28]. In the present study, steady-state and time-resolved fluorescence behavior of C-153 in ionic liquid and its mixture with water and methanol has been investigated basically to understand the interaction between the IL-water and IL-methanol binary mixtures and also to unravel the effect of these interactions on solute and solvent dynamics. 2-amino-7-nitroflurene (ANF) has been used for excitation wavelength dependence fluorescence measurements. Theoretical calculations have been carried out to understand the molecular origin of IL-cosolvent interaction. Molecular structural information of the BMIMTFA, C153 and ANF is provided in Scheme 1.

Experimental Section

Materials

Laser grade C153 was used as received from Exciton, USA. BMIMTFA (Scheme 1) was obtained from Merck, Germany (>99 % purity) and used as received. The water and halide contents of the ILs are <100 ppm. BMIMTFA were taken in different long-necked quartz cuvette and requisite amount of C153 was added to prepare the solution so that the optical density does not exceed 0.3. Proper precaution was maintained to avoid moisture absorption by this media during transferring the solute into the cuvette. The long-necked quartz cuvette was sealed with septum and parafilm to avoid moisture absorption form the environment. Millipore water was used as received which is purified in Merck, Mili-Q. HPLC grade methanol was obtained from Merck, Germany and used without further purification. Water and methanol were added as the cosolvents such that their molefractions were maintained at 0.4. The probability of dye aggregation was ruled out and it was confirmed from the spectroscopic study.

Instrumentation

The absorption and fluorescence spectra were collected using Cary 100 Bio spectrophotometer and Perkin Elmer, LS 55 spectrofluorimeter respectively. The fluorescence spectra were corrected for the spectral sensitivity of the instrument and samples were excited at 405 nm. Time-resolved fluorescence measurements were carried out using a time-correlated single-photon counting (TCSPC) spectrometer (Edinburgh, OB920) using a 405 nm picosecond laser diode (EPL), and the signals were collected at magic angle (54.7°) using a Hamamatsu microchannel plate photomultiplier tube (R3809U-50). The lamp profile is recorded by scatterer (dilute ludox solution in water) in place of the sample. The instrument response functions (IRF) of our TCSPC setup is 98 ps for 405 nm picoseconds diode laser which is measured by determining full width half maxima (FWHM) of lamp profile. Nonlinear least-squares iteration procedure was used for decay analysis using F900 decay analysis software. The qualities of the fit were judged by the chi square (χ^2) values and weighted deviations which are obtained by fitting. The same TCSPC instrument set up was used for anisotropy decay measurements. The emission intensities at parallel (I_{II}) and perpendicular ($I_{\perp}$) polarizations were collected alternatively until a peak difference between parallel (I_{II}) and perpendicular ($I_{\perp}$) decay (at t=0) ~5000 was reached. For G-factor calculation, the same procedure was employed, but with 5 cycles and horizontal polarization of the exciting laser beam. The same software was also used to analyze the anisotropy decay profile. The temperature was controlled by circulating water through the cell holder using a Quantum, North West (TC

Scheme 1 Structures of the RTIL 1-Butyl-3-methylimidazolium trifluoroacetate (BMIMTFA), 2-amino-7-nitrofluorene (ANF) and Coumarin 153 (C153)

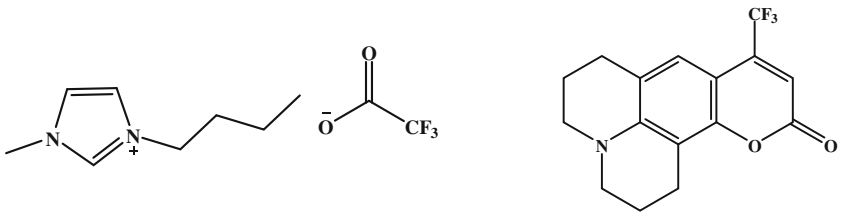

1-Butyl-3-methylimidazolium trifluoroacetate (BMIMTFA) **Coumarin 153 (C153)**

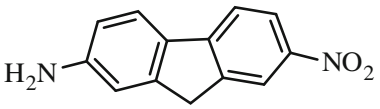

2-amino-7-nitroflurene (ANF)

125) temperature controller. LVDV-III Ultra Brookfield Cone and Plate viscometer (1 % accuracy and 0.2 % repeatability) was used for viscosity measurement of the IL.

Method

The time-resolved fluorescence decay profiles were collected at 5/10 nm intervals across the entire steady-state emission spectra at magic angle (54.7°). The total number of measurements was 25–30 in each case. Each decay curve was fitted by triexponential decay function after deconvoluting the instrument response function and the quality of the fit was judged by χ^2 values. The time resolved fluorescence decay profile was analyzed for constructing the time resolved emission spectra (TRES) using the standard method which is available in literature [28]. The peak frequencies obtained from the log-normal fitting of TRES were then used to construct the decay of solvent response function (*C (t)*) which is given below.

$$C(t) = \frac{\bar{\nu}(t) - \bar{\nu}(\infty)}{\bar{\nu}(0) - \bar{\nu}(\infty)} \tag{1}$$

Where $\bar{\nu}$ (∞), $\bar{\nu}$ (*0*) and $\bar{\nu}$ (*t*) are the peak frequencies at times infinity (∞), zero (*t* =0) and t respectively. Then the solvent response function was fitted by the following biexponential function

$$C(t) = a_1 e^{-t/\tau_1} + a_2 e^{-t/\tau_2} \tag{2}$$

Where $\tau_1$and $\tau_2$are the solvent relaxation time and a_1 and a_2 are normalized preexponential factors. After having the value of τ_1,τ_2, a_1, and a_2,the average solvation time were calculated by using the following relation

$$\langle \tau_{av} \rangle = a_1 \tau_2 + a_2 \tau_2 \tag{3}$$

We have also fitted *C(t)* to the stretched exponential function which is shown below.

$$C(t) = exp\left(-(t/\tau_{solv})^{\beta}\right) \tag{4}$$

where $0<\beta\leq 1$

$$\langle \tau_{st} \rangle = \frac{\tau_{solv}}{\beta} \Gamma\left(\beta^{-1}\right) \tag{5}$$

Where Γ is the gamma function and τ_{st} is the average solvation time considering *C(t)* is a stretched exponential function.

Geometry optimization calculations were performed by Gaussian 03 program [29] using density functional theory at the B3LYP/6-31++G(d, p) level of theory. This level of theory has been recently employed to understand the IL-cosolvent interaction by many groups [19, 30–32]. The optimized geometry is identified with lowest energy with no imaginary frequency.

Result and Discussion

Steady-State Spectral Measurements

Solute-solvent interactions in neat IL as well as IL-cosolvent mixtures have been studied by monitoring absorption and fluorescence measurements. C153 in neat BMIMTFA shows a broad absorption spectrum with a peak at 425 nm. The absorption and emission spectra of C153 in BMIMTFA along with emission spectrum of neat IL are shown in the Fig. 1. The emission maximum of C153 in this IL is found to be 532 nm, which closely matches with that in methanol [19]. The observation indicates that the polarity of BMIMTFA is close to that of methanol. Quite interestingly, the absorption and emission maximum of C153 remains almost unaffected when mole-fraction of co-solvents (water

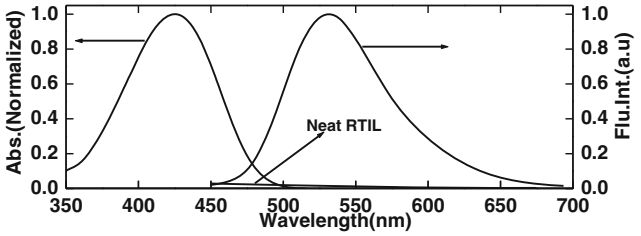

Fig. 1 Absorption and emission spectra of C153 in BMIMTFA. Emission spectrum of neat IL is also shown in the same figure

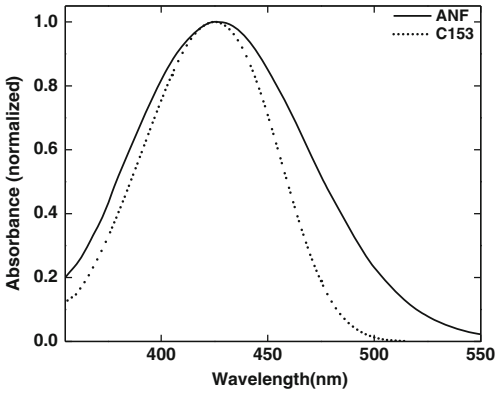

Fig. 2 Absorption spectra of ANF and C153 in BMIMTFA. Spectra are normalized by their respective peak values

and methanol) added to the neat IL independently is maintained at 0.4. This steady state spectral behavior also illustrates that the local polarity around the probe molecule is not affected by the given amount of highly polar solvents such as water and methanol.

In this context, it is pertinent to mention that ionic liquids are micro-heterogeneous in nature [33–44]. Micro-heterogeneous natures of ionic liquids [38–44] as well as deep eutectic melts [45, 46] are known to influence medium dynamics considerably. It has been pointed out that these liquids form microscopic polar and nonpolar domains and intermolecular interactions play an important role to their micro-heterogeneous behavior. In light of these it is also expected that IL-cosolvent mixture will also be micro-heterogeneous in nature. Infact, Biswas and Shiorota [14] investigated the microscopic aspects of ionic liquid-water systems by Raman and IR spectroscopy. They have shown that water aggregation is localized at ionic regions. It should be noted that the competition between the lifetime of these domains formed by IL-water and IL-methanol and the timescale of a particular chemical process taking place in these media, will eventually govern the rate of the chemical process induced by spatial heterogeneity of the medium. Moreover, temporal heterogeneity can also significantly modify the rate of a chemical process through dynamic solvent effects. In view of this, understanding the heterogeneity aspects of these media is extremely important. Since water and methanol are expected not to interact with the ionic liquid in the same manner it is expected that the medium heterogeneity exhibited by IL-water and IL-methanol would not be same.

In order to explore the micro-heterogeneous behaviour of the present solvent systems we have further carried out photophysical investigation by employing another dipolar probe 2-amino-7-nitrofluorene (ANF). The choice of ANF is governed by the fact that ANF has shorter excited state lifetime(τ) ~100 ps [38] than C-153 in conventional solvents, and hence it is expected that the former system would be more useful than the later in probing the micro-heterogeneous nature of ionic liquid [38]. In case of absorption, both ANF and C153 exhibits broad absorption band in BMIMTFA with full width at half maximum (FWHM) for ANF and C153 are 5421 cm $^{-1}$and 4168 cm $^{-1}$ respectively (Fig. 2). This observation indicates that there exists a distribution of molecules having different energies in the ground state. No significant change in the FWHM values between IL and IL-cosolvents has been observed. To throw more light on the micro-heterogeneous behaviour of IL and IL-cosolvents systems, we have also carried out excitation wavelength dependent fluorescence behaviour of ANF. Excitation wavelength dependent fluorescence behavior of ANF in IL-water and IL-methanol mixtures is shown in Fig. 3. As can be seen from Fig. 3, the variations of the λ_{max} of the fluorescence spectrum with the variation of the excitation wavelength are quite different for IL+ water from that of IL+ methanol. For example, the shift of λ_{max} of the fluorescence is found to be higher (3,400 cm^{-1}) in case of IL+ water system as compared to that (1,797 cm^{-1}) in IL+ methanol system. We would like to mention here that this observation of red shift of $\lambda_{em.}$(max) of the dipolar molecules when excited at the long-wavelength edge of the first absorption band, is known as "red-edge effect"(REE) [47, 48]. The REE effect in ILs have been rationalized by considering existence of a distribution of energetically different solvated probes in the ground state and a slower rate of their excited-state relaxation processes than the

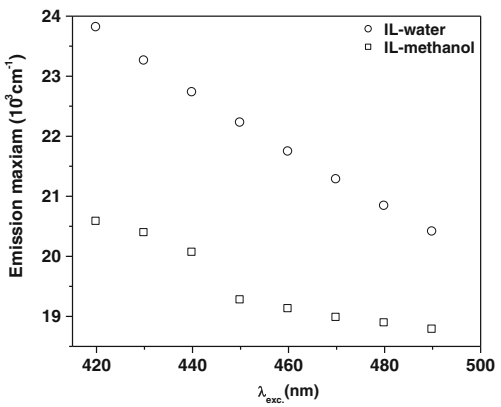

Fig. 3 Emission maxima (cm^{-1}) vs. $\lambda_{exc.}$ (nm) plots of ANF in IL-cosolvent systems at room temperature

excited lifetime (80–120 ps) [38]. The results obtained in the present study provide supports in favor of the spatial heterogeneity that exists in these IL-cosolvent mixtures. This observation also indicates that possibly the interplay of varying nature of intermolecular hydrogen-bonding interaction that exists between the anionic moiety of the IL and water and methanol is primarily responsible for the observed excitation wavelength dependent fluorescence behavior (REE) of the two mixtures.

Time Resolved Studies

Lifetime Measurements

In the present case we have also measured the excited state lifetimes of both ANF and C153 in neat IL and IL-cosolvents systems (Table 1). The data that are collected in Table 1 reveals that the average excited state lifetime (τ) values for ANF in the present solvent systems are much shorter (~80–120 ps) than that of C153 (3.5–4 ns). Interestingly, the measured excited state lifetime values for ANF (80–120 ps) are also found to be shorter than the measured average solvation time (200–350 ps) in these media (*vide* Table 2). Since slow *i.e.* incomplete relaxation of the fluorescent state is responsible for REE phenomenon [38], ANF is expected to be more suitable to exhibit stronger excitation wavelength dependent fluorescence behavior in the present case.

Dynamic Stoke's Shift Measurements

As stated in the "experimental section", the magic angle fluorescence decays of C153 are collected at 5–10 nm wavelength intervals covering the entire range of emission spectra. Wavelength-dependent decay profiles, which indicate typical signature of slow solvation dynamics, have been noticed in the present study. Representative wavelength dependent decay profile is shown in Fig. 4. for BMIMTFA-H_2O system. When emissions are monitored at shorter wavelength regions, only a faster decay is observed, and at the longer wavelengths, the decay profiles consist of a slow rise followed by the usual decay. TRES of C153 in BIMITFA-H_2O system at different time intervals are also shown in Fig. 5. A time-dependent shift of the emission spectra toward the lower energy confirms solvent-mediated relaxation of the excited state of the fluorophore. The representative plots of *C(t)* versus time for C153 shown in Fig. 6. for all these system. The average solvation times are estimated to be different for different systems (Table 2) and also found out to depend on co-solvent. For example, the average solvation times estimated to be 0.305, 0.224 ns in case of BMIMTFA-H_2O, BMIMTFA-CH_3OH systems respectively (Table 2).

Quite interestingly, the data collected in Table 2 also reveal that with the addition of same mole fraction of co-solvent, lowering of the viscosity is higher for methanol than that for water. It points out that methanol more effectively separates the cations and anions of IL than water causing relatively more decrease of cohesive energy between ions and eventually this result in more lowering of the bulk viscosity of the IL-methanol system [19]. This observation further indicates that IL interacts differently with methanol and water. As the medium viscosity profoundly influences solute dynamics, the average solvation time is found to be much less in case of BMIMTFA-CH_3OH system (Table 2). Table 2 also illustrates that the average solvation time drops more (1.64 times) in IL-methanol system than in IL-water system (1.20 times) even for the same mole-fraction of the respective co-solvents.

Rotational Diffusion of C153

The rotational dynamics of photo excited probe is very sensitive to microenvironment of the probe and local viscosity of the medium [27]. We have carried out the time resolved fluorescence anisotropy decay (TRAFD) of C153 in neat BMIMTFA, BMIMTFA-H_2O and BMIMTFA-CH_3OH media in order to know the effect of co-solvent addition on the microenvironment of photoexcited probe. Time-resolved fluorescence anisotropy decay (r (t)) is predicted by the following equation

$$r(t) = \frac{G\ I_{VV}(t) - I_{VH}(t)}{GI_{VV}(t) + 2I_{VH}(t)} \quad \text{Where } G = \frac{\sum I_{HH}(t)}{\sum I_{HV}(t)} \qquad (6)$$

where G is the instrument correction factor for the detector sensitivity to the polarization of the emission. It is 0.7 for our

Table 1 Time resolved fluorescence lifetime decay parameters for ANF and C153 in BMIMTFA, BMIMTFA-H_2O and BMIMTFA-CH_3OH systems

Probe	Systems	τ_1(ns)	τ_2(ns)	τ_3(ns)	$<\tau>$(ns)[a]
ANF	BMIMTFA	0.11(98.5 %)	0.68 (1.5 %)	–	0.118
	BMIMTFA-H_2O	0.06(98.2 %)	0.65(1.6 %)	4.54(0.2 %)	0.078
	BMIMTFA-CH_3OH	0.08(97.5 %)	0.55(2.3 %)	4.04(0.2 %)	0.099
C153	BMIMTFA	0.98(30.73 %)	5.34(69.27 %)	–	4.000
	BMIMTFA-H_2O	0.20(19.50 %)	1.45(22.40 %)	5.33(58.10 %)	3.460
	BMIMTFA-CH_3OH	0.56(21.50 %)	2.29(14.70 %)	5.55(63.80 %)	4.000

goodness of fit (χ^2) values are in between 1.0–1.2 and [a] experimental error is±5 %

Table 2 Solvent relaxation parameters of C153 in BMIMTFA, BMIMTFA-H_2O and BMIMTFA-CH_3OH systems

System	Vis.(cp)	Biexponential fit[a]					Stretched exponential fit[b]			Obs. Shift (cm^{-1})
		a_1	τ_1(ns)	a_2	τ_2(ns)	[c]$\tau_{av.}$(ns)	β	$\tau_{solv.}$(ns)	τ_{st}(ns)	
BMIMTFA	69	0.26	0.854	0.74	0.198	0.368	0.82	0.296	0.330	999
BMIMTFA- H_2O	37	0.19	0.887	0.81	0.168	0.305	0.82	0.235	0.262	1023
BMIMTFA-CH_3OH	26	0.29	0.458	0.71	0.128	0.224	0.84	0.192	0.210	899

[a] according to Eq. 3 and [b] according to Eq. 5. [c] experimental error ±5 %

TCSPC set up at the wavelength of detection. $I_{HH}(t)$ and $I_{HV}(t)$ is the intensity of fluorescence decays when the excitation and the emission polarizer are polarized at horizontal-horizontal and horizontal-vertical alignment respectively. Again $I_{VV}(t)$ and $I_{VH}(t)$ are the intensity of fluorescence decays when excitation and emission polarizer are polarized at vertical-vertical and vertical-horizontal alignment respectively. The time-resolved fluorescence anisotropy decay profile for BMIMTFA, BMIMTFA-H_2O and BMIMTFA-CH_3OH at $\lambda_{exc.}$ = 405 nm is shown in Fig. 7. The rotational relaxation parameters of C153 in neat RTIL and their cosolvent mixtures at different temperatures are shown in Table 3. The anisotropy decay profile are well fitted by biexponential function which is given below

$$r(t) = a_1 e^{-t/\tau_1} + a_2 e^{-t/\tau_2} \quad (7)$$

where a_1, a_2 are the amplitude and τ_1, τ_2 are the time constant. The average rotational relaxation time ($<\tau_r>$) was calculated by the following equation

$$\langle \tau_r \rangle = \frac{a_1\tau_1 + a_2\tau_2}{a_1 + a_2} \quad (8)$$

It can be seen from Table 3 that average rotation time of C153 in neat IL is 3.16 ns and C153 rotates faster as cosolvents are added to the neat ionic liquid. The faster rotation of C153 upon addition of cosolvent can be attributed to the lowering of the viscosity of the medium. However, quite interestingly, Table 3 also shows a more drop in average rotational time (1.98 ns) in IL-methanol systems than that (2.52 ns) of IL-water system. The observation indicates that the two solvents interact quite differently with the neat ionic liquid and thus induce different extent of structural heterogeneity to the medium. In this context, it is pertinent to mention that ionic liquids with alkyl chain C_4 or longer are known to be spatially heterogeneous in nature having polar and nonpolar domain [33–37, 44]. Nonpolar domain is believed to be formed mainly by aggregation of apolar alkyl chains, and polar domain forms because of the cations and anions [33–37, 44]. In light of this one can also reasonably assume that in case of the present ionic liquid, BMIMTFA, butyl chain would be responsible to form a nonpolar domain and the imidazolium cations and TFA anion would give rise to polar domain.

It is also expected that due to the presence of electrostatic and hydrogen binding interactions, the polar domain of BMIMTFA would be closely packed than the nonpolar region where only weak van der Waals interactions are present among the butyl chain. The nonpolar and polar domains are interconnected and give rise to organized network [27]. It is also expected that water and methanol would interact differently with the ionic liquid and thereby perturb the organized

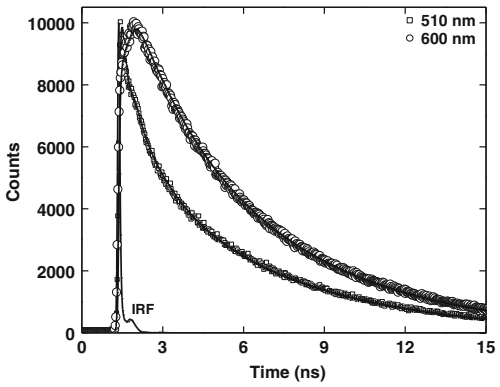

Fig. 4 Fluorescence decay profile of C153 in BMIMTFA-H_2O system at different monitoring wavelength. The monitoring wavelengths are shown by the corresponding symbol in the same figure. Instrument response function (IRF) of the TCSPC technique is also given in the figure. *Symbols* denote the data points and *solid lines* are fit to the data points

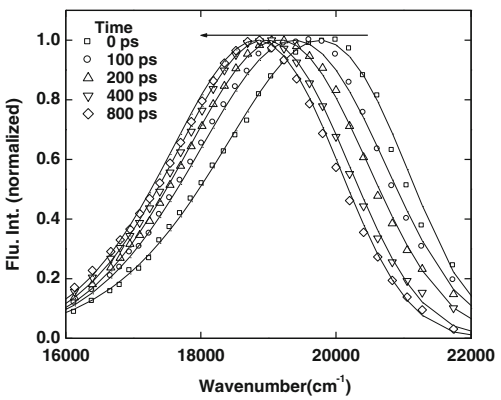

Fig. 5 Time resolved emission spectra (TRES) of C153 in BMIMTFA-H_2O system at different time spanned. *Symbols* denote the experimental data points and *solid lines* represent the log normal fit to the data points. The time intervals are shown by the *symbols* clearly in the same figure

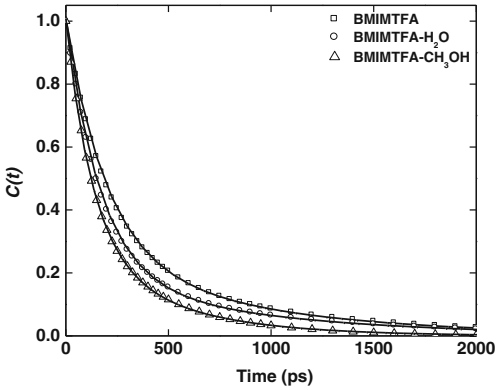

Fig. 6 Decay of solvent correlation function, *C(t)* of C153 in BMIMTFA, BMIMTFA-H_2O, BMIMTFA-CH_3OH systems. *Symbols* denote the experimental data points and *solid lines* represent the biexponential fit to the data points

network of ionic liquid which will eventually lead to a change in the microviscosity of the medium. As a result, rotational dynamics C153 is expected to be influenced which is also observed in the present case (Table 3).

To get a closer insight on whether the change in the organized structure affects the solute-solvent coupling, we have further analyzed the experimentally measured rotation time with the help of well known Stokes-Einstein-Debye (SED) hydrodynamic theory. According to this theory, the rotational movement of a medium sized solute molecule in a solvent continuum is implicit to occur by small step diffusion and its rotation time is correlated to the bulk viscosity of the solvent and temperature by the following relation

$$\tau_r^{SED} = \frac{\eta V f C}{k\ T} \tag{9}$$

Where k is the Boltzmann constant and T is absolute temperature. V is the van der Waals volume of the solute molecule, f is the shape factor and C is the boundary

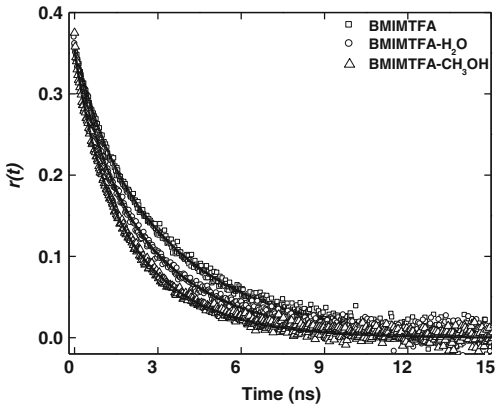

Fig. 7 Time resolved fluorescence anisotropy decay of C153 in BMIMTFA, BMIMTFA-H_2O, BMIMTFA-CH_3OH systems at 293 K. *Symbols* denote the experimental data points and *solid lines* represent the biexponential fit to the data points

condition parameter, which expresses the measure of coupling between the solute and solvent. The two extreme margin conditions are stick and slip according to SED hydrodynamic theory [49]. When the rotating solute molecule is larger in size than solvent molecule, C is close to unity and it denotes the stick boundary condition. In the case of a similar or smaller solute molecule than the molecule o the medium, C is less than unity. The shapes of the solute molecules are usually considered either to be symmetric or asymmetric ellipsoids in SED theory. For nonspherical molecules, f is greater than unity and the extent of deviation from unity in the value of f describes the degree of nonspherical nature of the rotating solute molecule. For the calculation of slip boundary condition (C_{slip}), C153 is considered as asymmetric ellipsoid to determine rotational time. For calculation of C_{slip}, we have taken the probe properties which are already available in literature [25]. Details of the procedure have been described in our earlier publications [50]. The van der Waals volume, shape factor, and calculated slip boundary condition parameter for C153 are 243 $Å^3$, 1.5, and 0.18 respectively [25, 50]. The slip and stick boundary limit, which have been assigned with the help of SED hydrodynamic theory are shown in the Fig. 8. with experimentally measured rotational time of C153 in neat BMIMTFA, BMIMTFA-H_2O and BMIMTFA-CH_3OH systems respectively. Quite interestingly, the last column of Table 3 reveals that solute-solvent coupling constant (C_{obs}) values are different for neat IL, IL-water and IL-methanol system. In case of neat IL, the C_{obs}values are found to be similar to the conventional solvents [51] whereas for other two mixtures it is found to be higher than for the neat ILs. The change in the C_{obs} values probably indicates a change in the organized structure of the ionic liquids upon cosolvent addition. Moreover, our observation on different C_{obs} values in presence of same molefraction of water and methanol indicates that water and methanol induce different heterogeneity to the neat IL by virtue of their varying nature of intermolecular interaction with IL.

Quantum Mechanical Calculation

To obtain the molecular origin of IL-colsolvent interactions, we have optimized the ground state structures of neat BMIMTFA, BMIMTFA-H_2O and BMIMTFA-CH_3OH systems at B3LYP/6-31++G (d, p) level of theory. As many conformers are possible for neat IL, lowest energy geometries are preferred for further (IL-cosolvent) calculation. The optimized geometries and structural parameters associated with them are provided in Fig. 9 and Table 4 respectively.

In the B3LYP/6-31++G (d, p) level optimized geometry of neat BMIMTFA the distance between H6-O32, H13-O31 are 1.745, 2.102 Å respectively. The van der waals O….H distance is 2.72 Å [52] which is higher than the observe

Table 3 Rotational relaxation parameters of C153 in BMIMTFA, BMIMTFA-H_2O and BMIMTFA-CH_3OH systems at different temperature

Systems	Temp.(K)	Vis.(cP)	[a]r_0	a_1	τ_1(ns)	a_2	τ_2(ns)	$<\tau_r$ (ns)$>$[b]	[c]$C_{obs.}$
BMIMTFA	293	69	0.37	0.18	0.86	0.82	3.67	3.16	0.52
	298	54	0.36	0.30	1.07	0.70	2.91	2.36	
	303	43	0.37	0.33	0.93	0.67	2.43	1.93	
	308	34	0.36	0.69	1.19	0.31	2.34	1.55	
	313	29	0.36	0.73	1.00	0.27	2.20	1.32	
BMIMTFA- H_2O	293	37	0.37	0.29	1.08	0.29	3.11	2.52	0.79
	298	30	0.35	0.20	0.52	0.80	2.30	1.94	
	303	24	0.35	0.29	0.72	0.71	2.02	1.64	
	308	20	0.36	0.53	0.80	0.47	2.20	1.37	
	313	16	0.34	0.54	0.75	0.46	1.69	1.18	
BMIMTFA- CH_3OH	293	26	0.37	0.29	0.80	0.71	2.47	1.98	0.84
	298	21	0.32	0.12	0.28	0.88	1.72	1.55	
	303	18	0.32	0.14	0.26	0.86	1.42	1.26	
	308	15	0.33	0.21	0.60	0.79	1.20	1.07	
	313	12	0.31	0.11	0.13	0.89	0.98	0.89	

[a] initial anisotropy and [b] average rotational time. [c] average rotational coupling constant

distance. The van der waals criteria for formation of X-H….Y bond is that the distance X….Y should be less than the sum of X-H covalent bond and the van der Waals radii of H and Y [53]. Angles among C3-H6-O32 and C11-H13-O31 are found to be 168°, 164° respectively. Considering distance and angle form the optimized geometry, it can be concluded that hydrogen bonding interaction exists between the imidazolium C_2-H proton and TFA anion. Methyl proton of imidazolium moiety is also found to make hydrogen bond with TFA anion (Fig. 9). Figure 9 also demonstrates the H-bonding interactions between IL-water and IL-methanol respectively. It has been observed that in case of water, the hydrogen atom of water molecule is hydrogen bonded to the O atoms of carboxylate moiety of IL with the distance 1.762 Å. A weak C-H…O interaction has also been observed between water oxygen atom and hydrogen atom of butyl chain. However, in case of methanol a shorter distance (1.699 Å) between methanol hydrogen and O atoms of carboxylate moiety of IL has been observed. C-H…O interaction between methyl hydrogen and oxygen atom of methanol is also found to be stronger as the distance between them is observed to be 2.041 Å which is shorter than the C-H…O distance (2.242 Å) in case of water (Fig. 9). We could not find any H-bonding interaction between imidazolium C_2-H proton and water/methanol within the 1:1 IL- cosolvent combination. It may be due to the fact that anion and water/methanol interaction is relatively stronger than that of imidazolium proton-water/methanol interaction. Steric factors may be also responsible for the absence of H-bonding between C_2-H proton of imidazolium and water/methanol. Almost Similar result is found in the optimized solution phase structure. All of these data indicate that the methanol is a better proton acceptor than water when it interacts with IL. These results imply that the replacement of H of water by methyl strengthens the H-bonding interactions and thus the interaction between methanol and ILs is stronger than the interaction between IL and water. In this context, it should be mentioned that geometries in Fig. 9 gives only most probable geometries of the complexes which only provide us the dominant interaction sites that exist between the constituents of the complexes.

From solvent and solute relaxation studies and the data obtained from theoretical calculations, it is evident

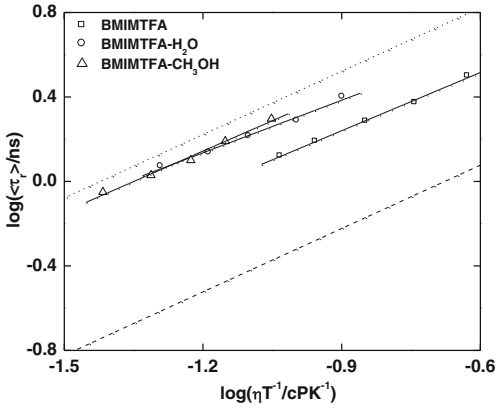

Fig. 8 log-log plots of rotational relaxation times of C153 vs. η/T in BMIMTFA, BMIMTFA-H_2O and BMIMTFA-CH_3OH system with slip and stick boundary condition parameters. *Dashed* and *dotted lines* represent the slip and stick boundary condition for C153. *Symbols* denote the experimental data points and *solid lines* represent the fit to the data points respectively

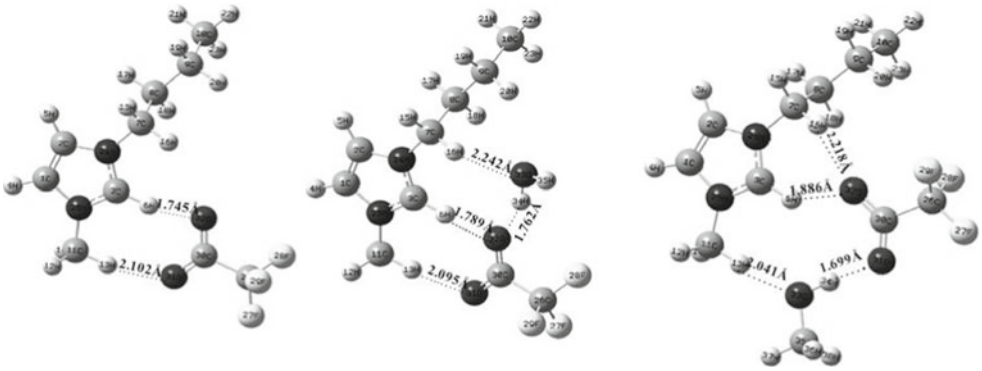

BMIMTFA BMIMTFA-H_2O BMIMTFA-CH_3OH

Fig. 9 Optimized structure of BMIMTFA, BMIMTFA-H_2O and BMIMTFA-CH_3OH system calculated at the B3LYP/6-31++G (d, p) level in the gas phase

from the present study that microscopic structural organizations are quite different for IL-water and IL-methanol systems. These data also lead us to conclude that the variation in structural reorganization is primarily responsible for the observed photophysical responses of C153 in these two media.

Table 4 Bond angle and bond distances from B3LYP/6-31++G (d, p) level of optimized structures of BMIMTFA, BMIMTFA-H_2O and BMIMTFA-CH_3OH systems in the gas as well as solution phase

System	Bond distances	(Å)		Bond angle	(°)	
		Gas phase	Solution phase		Gas phase	Solution phase
BMIMTFA	H6-O32	1.745	2.012	C3-H6-O32	168	179
	C3-H6	1.112	1.091			
	C3-O32	2.842	3.103			
	H13-O31	2.102	2.309	C11-H13-O31	164	175
	C11-H13	1.095	1.092			
	C11-O31	3.170	3.398			
BMIMTFA-H_20	H34-O32	1.762	1.819	O33-H34-O32	160	163
	O33-H34	0.984	0.980			
	O33-O32	2.708	2.773			
	H16-O33	2.242	2.390	O33-H16-C7	154	179
	C7-H16	1.093	1.093			
	O33-C7	3.260	3.483			
	H6-O32	1.789	2.027	O32-H6-C3	177	173
	C3-H6	1.106	1.086			
	C13-O32	2.894	3.110			
	H13-O31	2.095	2.380	O31-H13-C11	173	178
	C11-H13	1.096	1.092			
	C11-O31	3.185	3.471			
BMIMTFA-CH_3OH	H34-O31	1.699	1.770	O33-H34-O31	177	179
	O33-H34	0.994	0.986			
	O33-O31	2.756	2.756			
	H13-O32	2.041	2.204	C11-H13-O33	175	177
	C11-H13	1.096	1.092			
	C11-H33	3.134	2.295			
	H6-O32	1.886	2.123	C30-O32-H6	128	134
	C3-H6	1.096	1.085			
	C3-H32	2.838	3.103			
	H16-O32	2.218	2.504	C30-O32-H16	156	159
	C30-O32	1.257	1.092			
	C30-H16	3.408	3.449			

Conclusion

The present study has been carried out basically to understand the microscopic aspects of these two IL-cosolvent binary systems, BMIMTFA-H_2O and BMIMTFA-CH_3OH. We resort to steady state and time resolved fluorescence measurements as these studies effectively help to understand microscopic character of the medium. The photophysical measurements have been carried out by taking two dipolar probes C153 and ANF in neat BMIMTFA and its mixture with water and methanol. To understand the intermolecular interactions that exist between IL and IL-cosolvent systems, theoretical calculations have also been performed by optimizing the ground state geometries of BMIMTFA, BMIMTFA-H_2O and BMIMTFA-CH_3OH. Photophysical investigation reveals that water and methanol affects the solute and solvent dynamics in different ways. The present photophysical and theoretical calculations data possibly indicates that the varying nature of intermolecular interaction between IL and cosolvents induces different microscopic structural organization in the two binary systems.

Acknowledgments This work has been supported by the Department of Science and Technology (DST), Government of India. S. K. D. thanks the Council of Scientific and Industrial Research (CSIR), New Delhi for awarding fellowship. Thanks are due to National Institute of Science Education and Research (NISER), Bhubaneswar for awarding a fellowship to P. K. S.

References

1. Rogers RD, Seddon KR (2002) Ionic liquids industrial applications for green chemistry. Eds.; ACS Symposium Series 818; American Chemical Society: Washington, DC
2. Rogers RD, Seddon KR (2003) Ionic liquids as green solvent. Eds.; ACS Symposium Series 856; American Chemical Society: Washington, DC, Chapter 12
3. Rogers RD, Seddon KR (2005) Ionic Liquids IIIA: Fundamentals, progress, challenges, and opportunities: Properties and structure. Eds.; American Chemical Society: Washington, DC, Vol. 901
4. Judge RA, Takahashi S, Longenecker KL, Fry EH, Zapatero CA, Chiu ML (2009) The effect of ionic liquids on protein crystallization and X-ray diffraction resolution. Cryst Growth Des 9:3463–3469
5. Yao H, Zhang S, Wang J, Zhou Q, Dong H, Zhang X (2012) Densities and viscosities of the binary mixtures of 1-ethyl-3-methylimidazolium bis(trifluoromethylsulfonyl)imide with N-methyl-2-pyrrolidone or ethanol at T=(293.15 to 323.15) K. J Chem Eng Data 57:875–881
6. Fletcher KA, Pandey S (2003) Solvatochromic probe behavior within ternary Room-temperature ionic liquid 1-butyl-3-methylimidazolium hexafluorophosphate + ethanol + water solutions. J Phys Chem B 107:13532–13539
7. Widegen JA, Laesecke A, Magee JW (2005) The effect of dissolved water on the viscosities of hydrophobic room-temperature ionic liquids. Chem Commun 1610–1612. doi:10.1039/b417348a
8. Baker SN, Baker GA, Bright FV (2002) Temperature-dependent microscopic solvent properties of 'dry' and 'wet' 1-butyl-3-methylimidazolium hexafluorophosphate: correlation with $E_T(30)$ and Kamlet–Taft polarity scales. Green Chem 4:165–169
9. Harifi-Mood AR, Habibi-Yangjeh A, Gholami MR (2006) Solvatochromic parameters for binary mixtures of 1-(1-butyl)-3-methylimidazolium tetrafluoroborate with some protic molecular solvents. J Phys Chem B 110:7073–7078
10. Ficke LE, Brennecke JF (2010) Interactions of ionic liquids and water. J Phys Chem B 114:10496–10501
11. Jarosik A, Krajewski SR, Lewandowski A (2006) Conductivity of ionic liquids in mixture. J Mol Liq 123:43–50
12. Tokuda H, Baek SJ, Watanable M (2005) Room-temperature ionic liquids-organic solvent association: conductivity and ionic association. Electrochemistry 73:620–622
13. Masaki T, Nishikawa K, Shirota H (2010) Microscopic study of ionic liquid-H_2O systems: alkyl-group dependence of 1-alkyl-3-methylimidazolium cation. J Phys Chem B 114:6323–6331
14. Biswas R, Shirota H (2012) Intermolecular/interionic vibrations of 1 methyl-3 n octylimidazolium tetrafluoroborate ionic liquid and H_2O mixtures. J Phys Chem B 116:13765–13773
15. Chakrabarty D, Chakraborty A, Seth D, Hazra P, Sarkar N (2004) Dynamics of solvation and rotational relaxation of coumarin 153 in 1-butyl-3-methyl imidazolium hexafluorophosphate [bmim][PF_6]-water mixtures. Chem Phys Lett 397:469–474
16. Chakrabarty D, Chakraborty A, Seth D, Sarkar N (2005) Effect of water, methanol, and acetonitrile on solvent relaxation and rotational relaxation of coumarin 153 in neat 1-hexyl-3-methylimidazolium hexafluorophosphate. J Phys Chem A109:1764–1769
17. Paul A, Samanta A (2008) Effect of nonpolar solvents on the solute rotation and solvation dynamics in an imidazolium ionic liquid. J Phys Chem B 112:947–953
18. Pramanik R, Rao VG, Sarkar S, Ghatak C, Setua P, Sarkar N (2009) To probe the interaction of methanol and acetonitrile with the ionic liquid N, N, N-trimethyl-N-propyl ammonium bis (trifluoromethanesulfonyl)imide at different temperatures by solvation dynamics study. J Phys Chem B 113:8626–8634
19. Sarkar S, Pramanik R, Ghatak C, Setua P, Sarkar N (2010) Probing the interaction of 1-ethyl-3-methylimidazolium ethyl sulfate ([Emim][EtSO4]) with alcohols and water by solvent and rotational relaxation. J Phys Chem B 114:2779–2789
20. Daschakraborty S, Biswas R (2011) Stokes shift dynamics in (ionic liquid+polar solvent) binary mixtures: composition dependence. J Phys Chem B 115:4011–4024
21. Das SK, Sarkar M (2012) Steady-state and time-resolved fluorescence behavior of coumarin-153 in a hydrophobic ionic liquid and ionic liquid–toluene mixture. J Mol Liq 165:38–43
22. Carvalho PJ, Alvarez VH, Schroeder B, Gil AM, Marrucho IM, Aznar M, Santos LMNBF, Coutinho JAP (2009) Specific solvation interactions of CO_2 on acetate and trifluoroacetate imidazolium based ionic liquids at high pressures. J Phys Chem B113:6803–6812
23. Shiflett MB, Yokozeki A (2009) Phase behavior of carbon dioxide in ionic liquids: [emim][Acetate],[emim][Trifluoroacetate], and[emim][Acetate]+[emim][Trifluoroacetate] mixtures. J Chem Eng Data 54:108–114
24. Cammarata L, Kazarian SG, Salterb PA, Welton T (2001) Molecular states of water in room temperature ionic liquids. Phys Chem Chem Phys 3:5192–5200
25. Ito N, Arzhantsev S, Maroncelli M (2004) The probe dependence of solvation dynamics and rotation in the ionic liquid 1-butyl-3-methyl-imidazolium hexafluorophosphate. Chem Phys Lett 396:83–91
26. Jin H, Baker GA, Arzhantsev S, Dong J, Maroncelli M (2007) Solvation and rotational dynamics of coumarin 153 in ionic liquids: comparisons to conventional solvents. J Phys Chem B 111:7291–7302
27. Li B, Wang Y, Wang X, Vdovic S, Guo Q, Xia A (2012) Spectroscopic evidence for unusual microviscosity in imidazolium ionic

liquid and tetraethylene glycol dimethyl ether cosolvent mixtures. J Phys Chem B 116:13272–13281
28. Maroncelli M, Fleming GR (1987) Picosecond solvation dynamics of coumarin 153: the importance of molecular aspects of solvation. J Chem Phys 86:6221
29. Frisch MJ, Trucks GW, Schlegel HB, Scuseria GE, Robb MA, Cheeseman JR, Zakrzewski VG, Montgomery JA Jr, Stratmann RE, Burant JC, Dapprich S, Millam JM, Daniels AD, Kudin KN, Strain MC, Farkas O, Tomasi J, Barone V, Cossi M, Cammi R, Mennucci B, Pomelli C, Adamo C, Clifford S, Ochterski J, Petersson GA, Ayala PY, Cui Q, Morokuma K, Malick DK, Rabuck AD, Raghavachari K, Foresman JB, Cioslowski J, Ortiz JV, Stefanov BB, Liu G, Liashenko A, Piskorz P, Komaromi I, Gomperts R, Martin RL, Fox DJ, Keith T, Al Laham MA, Peng CY, Nanayakkara A, Gonzalez C, Challacombe M, Gill PMW, Johnson B, Chen W, Wong MW, Andres JL, Gonzalez C, Head-Gordon M, Replogle ES, Pople JA (2004) Gaussian 03, Revision C.02. Gaussian, Inc, Wallingford
30. Zhang QG, Wang NN, Yu ZW (2010) The hydrogen bonding Interactions between the ionic liquid 1-ethyl-3-methylimidazolium ethyl sulfate and water. J Phys Chem B 114:4747–4754
31. Wang NN, Zhang QG, Wu FG, Li QZ, Yu ZW (2010) Hydrogen bonding interactions between a representative pyridinium-based ionic liquid [BuPy][BF4] and water/dimethyl sulfoxide. J Phys Chem B 114:8689–8700
32. Zhang Q-G, Wang N-N, Wang S-L, Yu Z-W (2011) Hydrogen bonding behaviors of binary systems containing the ionic liquid 1-butyl-3-methylimidazolium trifluoroacetate and water/methanol. J Phys Chem B 115:11127–11136
33. Urahata SM, Ribeiro MCC (2004) J Chem Phys 120(4):1855–1863
34. Wang Y, Voth GA (2005) Unique spatial heterogeneity in ionic liquids. J Am Chem Soc 127:12192–12193
35. Lopes JNAC, Padua AAH (2006) Nanostructural organization in ionic liquids. J Phys Chem B 110:3330–3335
36. Lopes JNC, Gomes MFC, Padua AAH (2006) Nonpolar, polar, and associating solutes in ionic liquids. J Phys Chem B 110:16816–16818
37. Wang YT, Voth GA (2006) Tail aggregation and domain diffusion in ionic liquids. J Phys Chem B 110:18601–18608
38. Mandal PK, Sarkar M, Samanta A (2004) Excitation-wavelength-dependent fluorescence behavior of some dipolar molecules in room-temperature ionic liquids. J Phys Chem A 108:9048–9053
39. Jin H, Li X, Maroncelli M (2007) Heterogeneous solute dynamics in room temperature ionic liquids. J Phys Chem B 111:13473–13478
40. Adhikari A, Sahu K, Dey S, Ghosh S, Mandal U, Bhattacharyya K (2007) Femtosecond solvation dynamics in a neat ionic liquid and ionic liquid microemulsion: excitation wavelength dependence. J Phys Chem B 111:12809–12816
41. Das SK, Sarkar M (2012) Solvation and rotational relaxation of coumarin 153 in a new hydrophobic ionic liquid: an excitation wavelength dependence study. J Lumin 132:368–374
42. Das SK, Sarkar M (2012) Studies on the solvation dynamics of coumarin 153 in 1-ethyl-3-methylimidazolium alkylsulfate ionic liquids: dependence on alkyl chain length. ChemPhysChem 13: 2761–2768
43. Das SK, Sahu PK, Sarkar M (2013) Diffusion−viscosity decoupling in solute rotation and solvent relaxation of coumarin153 in ionic liquids containing Fluoroalkylphosphate (FAP) anion: a thermophysical and photophysical study. J Phys Chem B 117:636–647
44. Patra S, Samanta A (2012) Microheterogeneity of some imidazolium ionic liquids as revealed by fluorescence correlation spectroscopy and lifetime studies. J Phys Chem B 116:12275–12283
45. Pal T, Biswas R (2011) Heterogeneity and viscosity decoupling in (acetamide + electrolyte) molten mixtures: a model simulation study. Chem Phys Lett 517:180–185
46. Guchhait B, Daschakraborty S, Biswas R (2012) Medium decoupling of dynamics at temperatures ~100 K above glass-transition temperature: a case study with (acetamide + lithium bromide/nitrate) melts. J Chem Phys 136:11847
47. Valeur B, Weber G (1977) Anisotropic rotations in 1-naphthylamine. Existence of a red-edge transition moment normal to the ring plane. Chem Phys Lett 45:140–144
48. Weber G, Shinitzky M (1970) Failure of energy transfer between identical aromatic molecules on excitation at the long wave edge of the absorption spectrum. Proc Natl Acad Sci U S A 65:823–830
49. Hu CM, Zwanzig R (1974) Rotational friction coefficients for spheroids with the slipping boundary condition. J Chem Phys 60: 4354
50. Das SK, Sarkar M (2012) Rotational dynamics of coumarin-153 and 4-aminophthalimide in1-ethyl-3-methylimidazolium alkylsulfate ionic liquids: effect of alkyl chain length on the rotational dynamics. J Phys Chem B 116:194–202
51. Horng M-L, Gardecki J, Maroncelli M (1997) Rotational dynamics of coumarin 153: time-dependent friction, dielectric friction, and other nonhydrodynamic effects. J Phys Chem A 101:1030–1047
52. Bondi A (1964) van der Waals Volumes and Radii. J Phys Chem 68:441–451
53. Rahim Z, Barman BN (1978) The van der Waals Criterion for hydrogen bonding. Acta Crystallogr A 34:761–764